Estimation Of Subdaily Polar Motion With The Global Positioning System During The Epoch '92 Campaign

R. Ibanez-Meier[1, 2], A. P. Freedman[1], T. A. Herring[3], R. S. Gross[1], S. M. Lichten[1], U. J. Lindqwister[1]

Abstract. Data collected over six days from a worldwide Global Positioning System (GPS) tracking network during the Epoch '92 campaign are used to estimate variations of the Earth's pole position every 30 minutes. The resulting polar motion time series is compared with estimates derived from very long baseline interferometry (VLBI) observations. A time domain comparison of the semidiurnal and prograde diurnal frequency bands yields better than 0.3 milliarcsecond (mas) rms scatter between the series. Additional comparisons of these series with two models for polar motion variations at tidal frequencies suggest that most of the periodic subdaily fluctuation in the polar motion signal can be attributed to ocean tides. Both GPS and VLBI appear to measure the x-component of polar motion better than the y-component, probably a result of the uneven geographic station coverage by either technique.

1 ntroduction

Observations of the motion of the pole have a long history (see, for example, *Lambeck* [19S0], Eubanks [1993], and references therein). Polar motion, which is the movement of the Earth's rotation axis with respect to its crust, is a dynamic response of the Earth forced by its interactions with other celestial bodies and its own internal dynamics. The periods involved range from a nearly secular trend believed to result from post-glacial rebound, through the Chandler wobble period, and annual and shorter periods excited primarily by atmospheric motions, down to at least diurnal and semidiurnal periods resulting from the exchange of angular momentum between the oceans and the solid Earth. Angular momentum changes in the oceans at these daily and subdaily periods are of tidal origin, a product of both the equilibrium and non-equilibrium response of the world's oceans to the tidal potential at high frequencies [*Seiler, 1991;* Gross, 1993; *Wunsch and Seiler, 1992, Brosche and Wünsch,* 1994].

Polar motion is defined as the location of the rotation axis (or, more exactly, of the Celestial Ephemeris Pole) with respect to a geographic, crust-fixed, reference point such as the International Earth Rotation Service (IERS) reference pole [*McCarthy,* 1992]. It is described using two coordinates, polar motion *x* (PMX) and polar motion y (PMY), where the x-axis lies along the Greenwich meridian orthogonal to the reference pole z-axis, and the y-axis lies 90 degrees to the west.

Since the tendency in polar motion is towards decreasing amplitudes at shorter periods, an increase in sensitivity has been necessary to detect pole position changes at high frequencies. Space-geodetic techniques such as VLBI and satellite laser ranging (SLR) have played a prominent role in their study. Recently, *Herring et al. [1991]* and

[1] Jet Propulsion Laboratory, California Institute of Technology, Pasadena.

[2] Now at Wall Street Analytics, Palo Alto, CA.

[3] Department of Earth, Atmospheric, and Planetary Sciences, Massachusetts Institute of Technology, Cambridge.

Lindqwister et al. [1992] obtained daily GPS polar motion estimates in agreement with VLBI at the 0.5 mas (1.5 cm) level (rms) or better, Since then, several GPS processing centers have been routinely reporting daily estimates of pole position as part of the International GPS Service for Geodynamics (IGS).

Subdaily polar motion studies have been performed with VLB1 *[Herring and Dong*, 1994] and SLR [Watkins *and Eanes*, 1994] by estimating the amplitudes and phases of signals appearing at the well known frequencies of the tides. In this letter, we report instead on a time-domain study of subdaily GPS-derived polar motion measurements, and compare them with both VLBI estimates of polar motion and polar motion fluctuations expected at tidal frequencies. The data were collected during the intensive observing period known as Epoch '92 (part of the SEARCH '92 campaign organized by the IERS *[Dickey,* 1993]) during which time continuous and high-time resolution data were obtained by both VLBI and GPS.

Data Sets and Estimation Strategies

Data from 25 globally distributed GPS Rogue receivers tracking 17 GPS satellites from July 26 through July 31, 1992, were processed with the Jet Propulsion Laboratory's (JPL) GIPSY-OASIS 11 software. The data arc could not span more contiguous days due to anti spoofing (AS) signal encryption on August 1-2 and the consequent loss of data acquisition (improvements in software and hardware have since overcome this problem). The JPL software and standard JPL GPS estimation strategies, incorporating Kalman filtering, are described in detail by *Lichten [1990a,* 1990b] and *Blewitt [1993].*

GPS orbit states and three solar radiation parameters corresponding to three orthogonal flux components were estimated for each satellite. Earth orientation parameters were also estimated, with the IERS Bulletin B time series used as the source. for nominal values. Earth rotation (UT 1 R - UTC) variations were estimated every 30 minutes starting from an initial fixed value by using first-order Markov process updates with a correlation time of 4 hours and a steady-state process noise l-sigma constraint of 0.06 ms *[Freedman et al.,* 1994]. Station geocentric coordinates, except those for up to 8 fiducial (fixed) sites, were estimated as constants over the entire six day period, with ITRF 1991 coordinates [*Boucher et al.,* 1992] used as a priori station locations. The zenith troposphere delay at each receiver site was modeled as a random walk process. The 1980 International Astronomical Union (I AU) nutation model, the *Yoder et al. [1981]* model for tidal UT], and the GEMT3 gravity field model, were all employed. In addition, GPS carrier phase biases were estimated as real-valued parameters, and clock biases for transmitters and receivers were estimated as white noise processes, except for one reference station clock.

As observed by *Lindqwister et al. [1992],* changing fiducial stations induces only bias changes in our polar motion series, consistent with small rigid-body rotations of the reference frame. The pole position variability remained nearly invariant even in the absence of fiducial sites.

Two different estimation strategies for the satellite orbits were employed. In our first strategy, originally described in *Lichten and Bertiger [1989]* and *Lichten [1990a],* the solar radiation pressure coefficients Gx, Gy, and Gz were estimated as constants, with 10 percent colored noise added and updated every hour. The biases for the Gx and Gz parameters were constrained to be 100% correlated. The stochastic portion of the solar radiation model consisted of a first-order Gauss-Markov process with a correlation time of 4 hours. We found that this strategy, although adequate for estimating UT1R – UTC variations *[Freedman, et al., 1994],* tended to attenuate much of the polar motion signal, presumably absorbing it within the satellite orbit and solar pressure force models.

A second strategy, discussed by *Lichten et al. [* 1992], has proven better for polar motion estimation. In it, we re-estimated each satellite state (position, velocity and solar radiation pressure coefficients) every 24 hours as constant over the estimation interval. The white noise restarts for each GPS satellite were staggered over a 5 hour interval around noon to maintain continuity in the UT1 series.

With this estimation strategy for the orbits, we tried a variety of strategies for polar motion and found that unconstrained white noise estimates, every 30 minutes or less, gave consistent results in the prograde diurnal and semidiurnal bands discussed below. Typical postfit rms residuals were close to 6 mm for carrier phase and 35 cm for pseudorange data.

The VLBI series used for comparison in this study was generated from data acquired by three different VLB1 networks: “NASA R&D”, “IRIS” and “NAVNET” (see *Freedman et al. [1994]* for more details), Estimates were obtained with the NASA/GSFC, CFA/MIT-developed Kalman filter programs CALC and SOLVK *[Herring et al., 1990; Ma et al., 1992].* UTl, polar motion, nutation corrections, and station troposphere parameters were estimated over 24-hour time spans, with UT], polar motion and troposphere parameters modeled as random walks. Polar motion was estimated every 2 hours with 1.2 mas 1-sigma resets. The daily sets of polar motion estimates were concatenated to generate a 6-day time series. On days when two networks collected data, the less noisy data set was used. Use of the noisier data set does not significantly change the results of this study, however-,

We have also compared the GPS and VLB1 series to two independent models for polar motion variations at diurnal and semidiurnal tidal frequencies. The first, referred to as the Brosche-Seiler-Gross (BSG) tide model *[Gross,* 1993], is a theoretical model based on the oceanic angular momentum model of *Seiler* [1991*].* The BSG model accounts for the presence of the free core nutation of nearly diurnal retrograde frequency, which cannot be neglected at daily and subdaily frequencies. The second model used for comparison, referred to as the HD tide model *[Herring and Dong,* 1994], *is* an empirically determined model of polar motion fluctuations at tidal frequencies based on eight years of VLBI observations. Because it is empirical rather than theoretical, this model may contain periodic signals other than those due to ocean tides, coming, for instance, from the atmosphere. These two models tend to bracket the range of tidal polar motion models obtained by several other groups (see *Herring and Dong [1994]* for a recent summary).

Results and Discussion

As is well known, the retrograde diurnal motion of the pole is degenerate with long period nutation; hence, estimates of subdaily polar motion can be contaminated by nutation model errors (see *Eubanks [1,993]* for a lucid discussion). This is a result of retrograde diurnal polar motion being nearly fixed in Earth-centered inertial coordinates. Similarly, mismodeled orbital variations in the GPS constellation that appear slow in an inertial frame can be readily absorbed by the retrograde diurnal component of polar motion. To avoid ambiguities from these error sources, we removed the retrograde diurnal band in our comparisons with VLBI and tide model data sets. (The VLBI polar motion data already have little power at retrograde diurnal periods owing to the explicit estimation of nutation corrections in the VLBI estimation strategy,)

In Figure 1, we show the power spectrum of the GPS polar motion series estimated every 30 minutes with loose (120 mas) constraints. The large retrograde diurnal peak at -1 cycle/day (cpd) is contaminated by nutation and orbit modeling errors. The spectrum clearly shows peaks in the semi diurnal (±2 cpd) and prograde diurnal (+1 cpd) bands, with more subdued power elsewhere. To facilitate comparison with the tide models, it is these +1 cpd and ±2 cpd bands of the GPS time series on which we focus. These bands are studied in two ways: by explicit estimation of the spectral components from the Fourier transform of the original time series, and by filtering the geodetic and tide model time series with a 0.4 cpd fullwidth bandpass filter atrout the tidal bands.

Figure 2 illustrates the effects of this filtering on the GPS polar motion series. It shows the motion of the full (i.e., nominal plus estimate) polar motion vector over the six days. The original GPS series is quite noisy, jiggling around at the 1 mas level. (Note that formal errors of the GPS estimates range from 0.2 to 0.3 mas.) Removing only the retrograde diurnal term (at -1 cpd) does not alter the character of this variability. Retaining only the + 1 and ±2 cpd bands yields a much smoother curve which can more easily be compared with VLBI and the tide models.

We have found that much of the non-periodic, "noise" signature in our GPS and VLBI polar motion series varies significantly with estimation strategy. Thus, we have so far not been able to identify with confidence any signatures outside of the semidiurnal and prograde diurnal bands as real signals and not potential artifacts of our estimation strategy and/or models. The effect of this large noise component is shown in Figure 3. The raw VLBI and GPS series do not appear very much alike, but this is a result of the power in each series outside of the tidal bands. (Note also that prominent excursions in the VLBI time series, in particular, are associated with larger formal errors from less robust VLBI networks.) When bandpass filtered, agreement between the two series is readily apparent. We have therefore restricted further comparisons in this study to the semidiurnal (both prograde and retrograde) and diurnal prograde frequency bands.

Figure 4 illustrates the amplitude and phase of the spectral components of all four series in the three frequency bands. The tide model components are not the true model amplitudes and phases used to generate the time series, but rather the amplitudes and phases recovered from the spectral fit to the time series, thus more accurately reflecting the errors inherent in recovering the tidal bands from the geodetic series. The short length of the time series (less than 6 days) produces a spectral component spacing of 0.17 cpd, yielding two spectral peaks within each 0.4 cpd width band. Each peak is shown separately in Fig. 4. In most cases, the two tide models exhibit consistent amplitude-phase vectors. (The confidence level of each point is no better than about ±0.05 mas in the radial (amplitude) component and ±10° in the angular (phase) component.) The GPS and VLBI components agree reasonably well in all but the prograde semidiurnal (+2 cpd) band. The GPS solution agrees with the tide models particularly well in the +1 cpd band and moderately well in the -2 cpd band. VLBI is much more consistent with the tide models in the +2 cpd band than is GPS. The poor showing of GPS for this band may be due, in part, to the fact that the amplitude expected of this term is much smaller than the amplitudes of the other bands, and that the approximately 12-hour orbits of the GPS satellites might well lead to poorer results at semidiurnal frequencies.

Figure 5 shows time-domain PMX and PMY plots of the bandpass filtered GPS, VLBI, HD model, and BSG tide model time series. The rms differences between the VLBI and GPS series are 0.17 and 0.29 mas in PMX and PMY, respectively. The overall level of agreement in both amplitude and phase is noteworthy, particularly in the *x*-component. RMS differences between the various series plotted in Fig. S are given in Table 1; also listed are the series cross-correlations. The y-correlations are routinely smaller than the x-correlations. This is probably a result of both GPS and VLBI having weaker sensitivity to the *y* component of polar motion due to the uneven geographic coverage of ground stations for both techniques. The last line of Table 1 shows the poor agreement between the raw, unfiltered series, illustrating the importance of bandpass analysis for these data sets.

Our results suggest that most of the power in both the GPS and VLBI time series can be attributed to ocean tides. Better overall agreement in the x-component than the y-component is probably a result of poor station geometry for measuring PMY (e.g., a dearth of sites in Central Asia and the Indian Ocean), Subdaily polar motion estimates derived with GPS data are also highly sensitive to GPS orbit modeling strategies.

The polar motion results presented here are very encouraging, and are consistent with similar good agreement bet ween GPS and VLBI estimates of subdaily UT1 variability *[Freedman et al,, 1994]*. Longer data spans with corroborating VLBI observations should allow for more precise and accurate comparisons, as well as for the extension of this research outside the tidal bands. In this direction, we hope that this study will help in part to motivate future intensive VLB1 campaigns to provide high-quality data for intercomparison with GPS.

Acknowledgments. We are grateful to B. Haines, G. Hajj, 1., Rornans, and R. Muellerschoen for enlightening discussions, and to J. Dickey and J.A. Steppe for many helpful suggestions regarding this manuscript. The work of RIM, APF, SML, UJL, and RSG described in this paper was carried out by the Jet propulsion Laboratory, California Institute of Technology, tinder contract with the National Aeronautics and Space Administration (NASA). The work of TAH was supported by NASA under grant NAG 5-538 and NAW-0037, by the National Oceanic and Atmospheric Administration under grant NA90AA-D-AC481, and by the Kerr-McGee Foundation.

References

Blewitt, G., Advances in Global Positioning System technology for geodynamics investigations: 1978-1992, in *Contributions of Space Geodesy to Geodynamics: Technology,* edited by D. E. Smith and D. L. Turcotte, pp. 195-213, Am, Geophys. Un., Washington, D.C., 1993.

Brosche, P., and J. Wünsch, On the "rotational angular momentum" of the oceans and the corresponding polar motion, *Astron Nachr., 315, 181-188, 1994.*

Boucher, C., Z. Altamimi, and L, Duhem, ITRF 91 and its associated velocity field, *IERS Tech. Note 12,* Cent. Bur. of IERS, Ohs, de Paris, 1992.

Dickey, J. O., High time resolution measurements of Earth rotation, in *Advances in Space Research, 13,* pp. (11) 18S-(1 1)196, Pergamon, 1993.

Eubanks, T. M., Variations in the orientation of the Earth, in *Contributions of Space Geodesy to Geodynamics: Earth Dynamics*, edited by D. E. Smith and D. L. Turcotte, pp. 1 -S4, Am Geophys. Un., Washington, D. C., 1993.

Freedman, A. P., R. Ibañez-Meier, T. A. Herring, S. M. Lichten, and J. O. Dickey, Subdaily Earth rotation during the Epoch '92 campaign, *Geophys. Res. Lett., 21*, 769-772, 1994.

Gross, R. S., The effect of ocean tides on the Earth's rotation as predicted by the results of an ocean tide model, *Geophys. Res. Lett.*, 20, 293-296, 1993.

Herring, T. A., and D. Dong, Measurement of diurnal and semidiurnal rotation variations and tidal parameters of the Earth, *J. Geophys. Res.*, in press, 1994.

Herring, T. A., J. L. Davis, and 1.1. Shapiro, Geodesy by radio astronomy: The application of Kalman filtering to very long baseline interferometry, *J. Geophys. Res.*, 95, 12561-12581, 1990.

Herring, T. A., D. Dong, and R. W. King, Submilliarcsecond determination of pole position using Global Positioning System data, *Geophys. Res. Lett.*, 18, 1893-1897, 1991.

Lambeck, K., *The Earth's Variable Rota[ion: Geophysical Causes and Consequences, 449* pp., Cambridge University Press, New York, 1980.

Lichten, S. M., Toward GPS orbit accuracy of tens of centimeters, *Geophys. Res. Lett., 17,* 215-218, 1990a.

Lichten, S. M., Estimation and filtering for high-precision GPS positioning applications, *Man. Geod.*, 15, 159-176, 1990b.

Lichten, S. M. , and W. L Bertiger, Demonstration of sub-meter GPS orbit determination and 1.5 parts in 10^8 three-dimensional baseline accuracy, *Bul. Geod.*, 63, 167-189, 1989.

Lichten, S. M., S. L. Marcus, and J. O. Dickey, Sub-daily resolution of Earth rotation variations with Global Positioning System measurements, *Geophys. Res. Lett.*, 19, 537-540, 1992

Lindqwister, U. J., A. P. Freedman, and G. Blewitt, Daily estimates of the Earth's pole position with the Global Positioning System, *Geophys. Res. Lett.*, 19,845-848, 1992.

Ma, C., J. W. Ryan, and D. S. Caprette, Crustal Dynamics Project data analysis-1991 VLBI geodetic results, in *Nasa Tech. Memo 104552,* NASA - Goddard Space Flight Center, Greenbelt, MD, 1992.

McCarthy, D. D. (ed.), IERS Standards, *IERS Technical Note 13,* Cent. Bur. of IERS, Ohs. de Paris, 1992.

Seiler, U., Periodic changes of the angular momentum budget due to the tides of the world ocean, *J. Geophys. Res.*, 96, 10,287-10,300, 1991.

Watkins, M. M., and R. J. Eanes, Diurnal and semidiurnal variations in Earth orientation determined from LAGEOS laser ranging, *J. Geophys. Res.*, in press, 1994.

Wunsch, J., and U. Seiler, Theoretical amplitudes and phases of the periodic polar motion terms caused by ocean tides, *Astron. Astrophys., 266,581-587, 1992.*

Yoder, C. F., J. G. Williams, and M. E. Parke, Tidal variations of Earth rotation, *J. Geophys. Res.*, 86,881-891, 1981.

Table 1. RMS Differences and Correlations

	x rms (mas)	y rms (mas)	x corr.	y corr.
VLBI versus GPS	0.17	0.29	0.90	0.55
HD Model versus GPS	0.21	0.25	0,84	0.63
BSG Model versus GPS	0.26	0.36	0.78	0.21[a]
HD Model versus VLBI	0.25	0.21	0.80	0,77
BSG Model versus VLBI	0.26	0.26	0.79	0.68
HD Model versus BSG Model	0.25	0.24	0.81	0.69
Unfiltered VLBI versus unfiltered GPS	0.80	0.83	0.27’	0,25”

[a] This correlation is not statistically significant; all others are significant at above the 99.970 level.

Figure Captions

Fig. 1. GPS polar motion amplitude spectrum. The retrograde diurnal band is shown hatched, while the prograde diurnal and semidiurnal bands are shaded. Bandpass filtering attenuates the signal outside of the shaded regions,

Fig. 2. PMY versus PMX for the GPS data before filtering, after removing the retrograde diurnal band, and after bandpass filtering. The polar motion estimates have had their nominal values added.

Fig. 3. Comparison of the unfiltered GPS and VLBI residual polar motion time series (after removing the same reference series from both full polar motion series) with the bandpass filtered time series. The formal errors for the two unfiltered series are shown at the top. The series have been offset for visibility.

Fig. 4. Amplitude-phase diagrams of the spectral components of the GPS, VLBI, HD model, and BSG model time series. The two components in each band are shown separately. Typical uncertainty levels are ±0.05 mas in the radial direction, ±10° in the angular direction.

Fig. 5. (a) Bandpassed PMX time series of the GPS, VLBI, HD model, and BSG tide mode] data. (b) Same as (a), but for PMY.

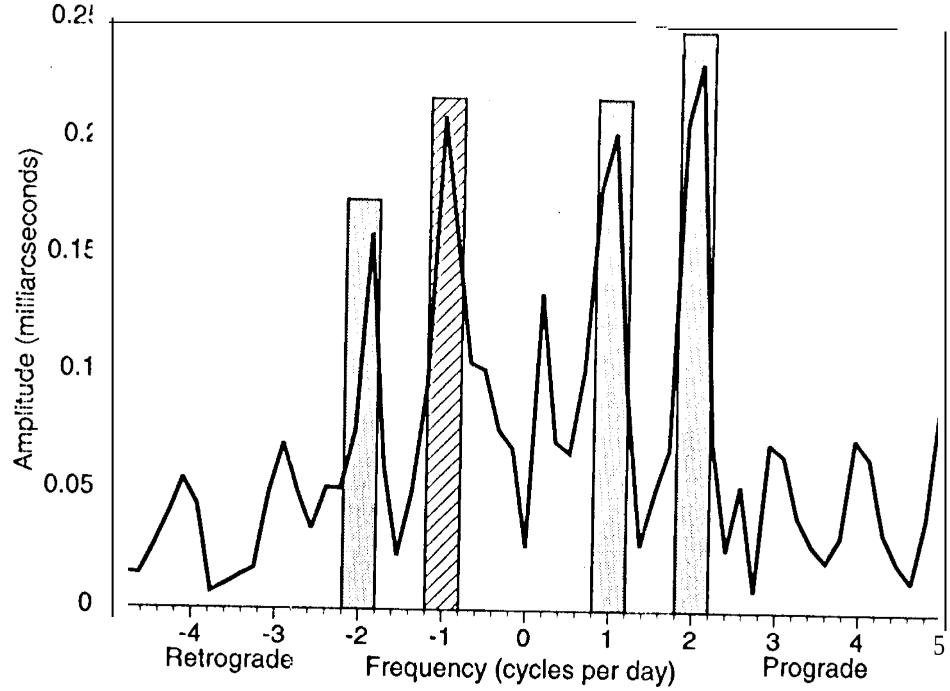

Figure 1.

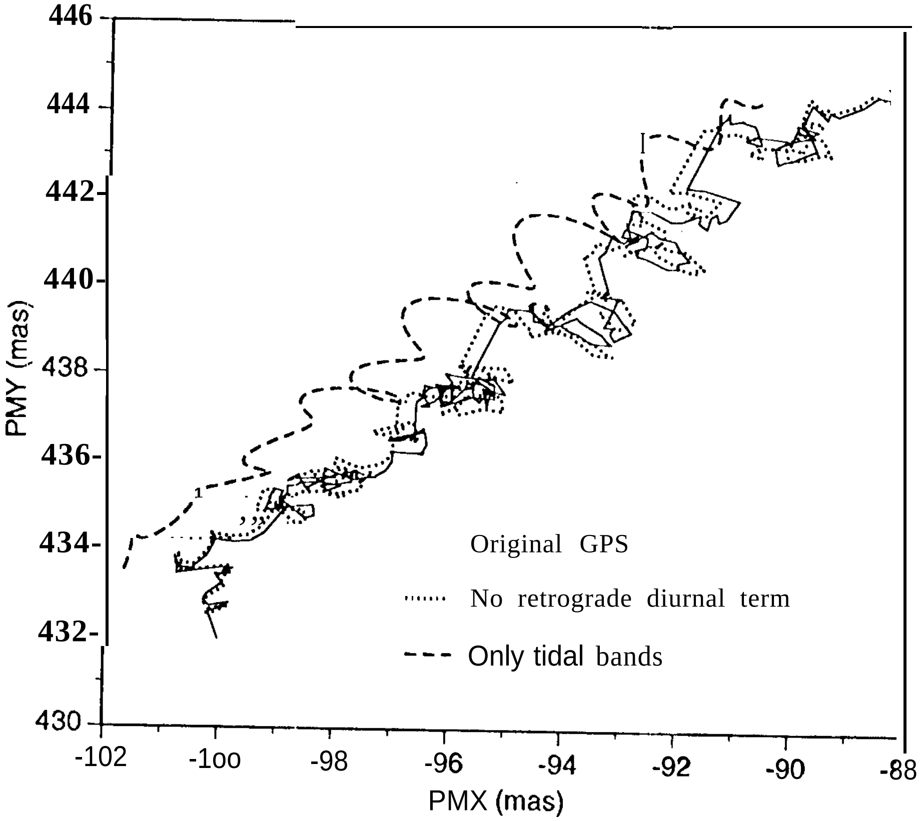

Figure 2.

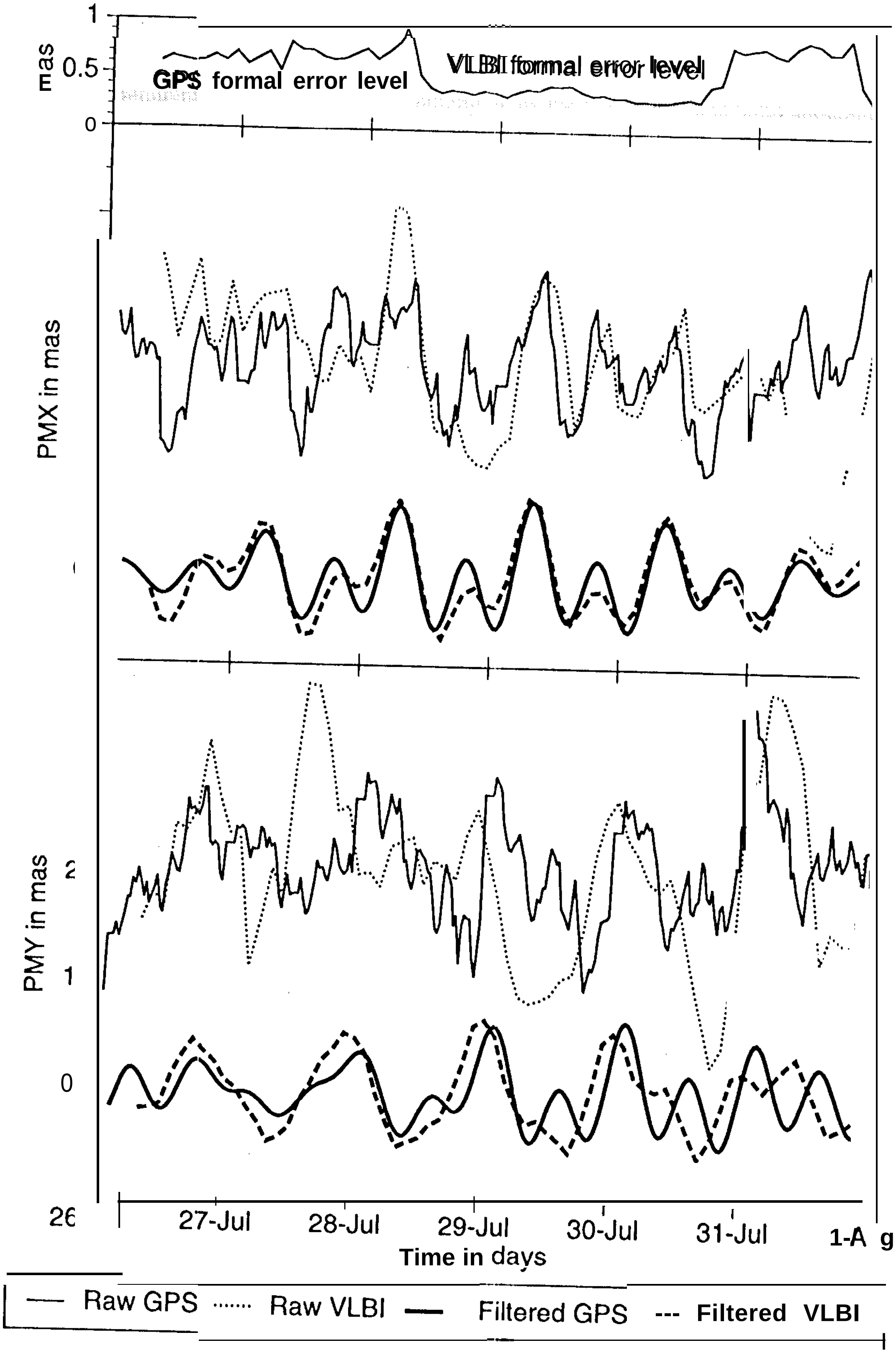
mas
1
0.5
0
GPS formal error level
VLBI formal error level
PMX in mas
PMY in mas
2
1
0
26
27-Jul
28-Jul
29-Jul
30-Jul
31-Jul
1-A g
Time in days
Raw GPS
Raw VLBI
Filtered GPS
Filtered VLBI

Figure 3.

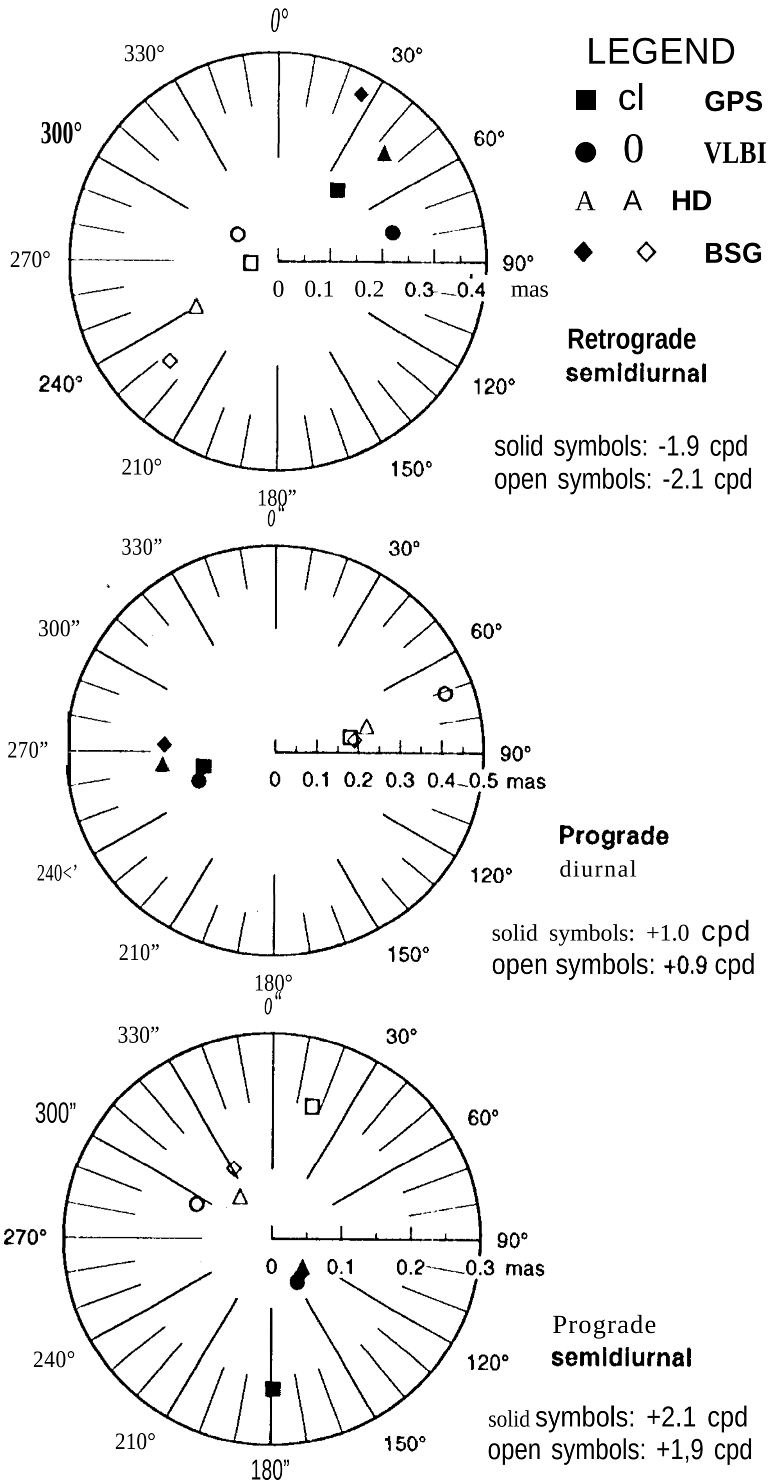

LEGEND
cl GPS
0 VLBI
A A HD
BSG
0°
30°
60°
90°
120°
150°
180”
210°
240°
270°
300°
330°
0 0.1 0.2 0.3 0.4 mas
Retrograde
semidiurnal
solid symbols: -1.9 cpd
open symbols: -2.1 cpd
0"
330”
30°
60°
300”
270”
90°
0 0.1 0.2 0.3 0.4 0.5 mas
240<’
120°
210”
150°
180°
Prograde
diurnal
solid symbols: +1.0 cpd
open symbols: +0.9 cpd
0"
330”
30°
300”
60°
270°
90°
0 0.1 0.2 0.3 mas
240°
120°
210°
150°
180”
Prograde
semidiurnal
solid symbols: +2.1 cpd
open symbols: +1,9 cpd

Figure 4.

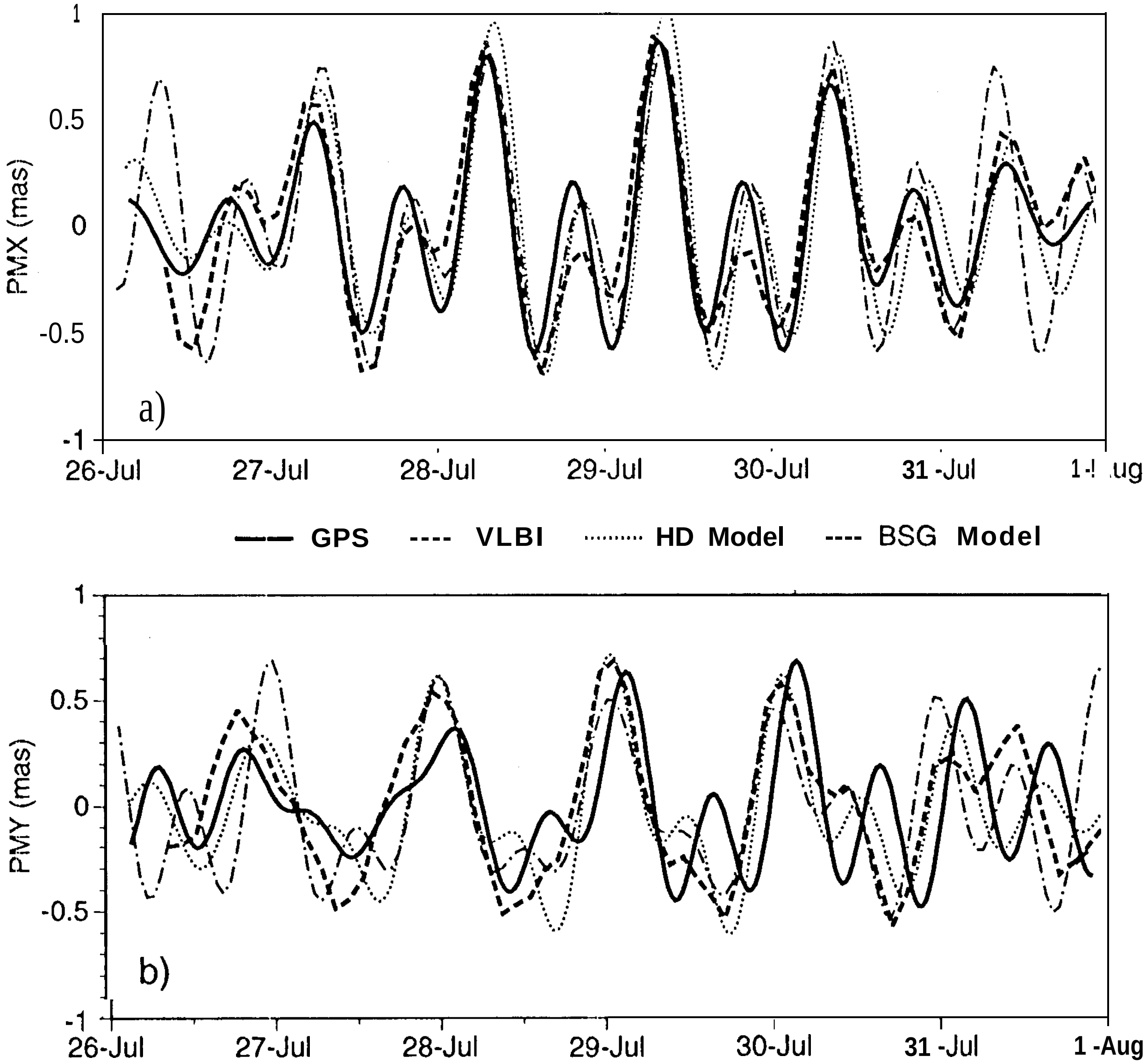
1
0.5
0
-0.5
-1
PMX (mas)
a)
26-Jul
27-Jul
28-Jul
29-Jul
30-Jul
31 -Jul
GPS
VLBI
HD Model
BSG Model
1
0.5
0
-0.5
-1
PMY (mas)
b)
26-Jul
27-Jul
28-Jul
29-Jul
30-Jul
31 -Jul
1 -Aug

Figure 5 a,b.